Acc. Chem. Res. **2002,** *35,* 1008−1017

Multiwall Carbon Nanotubes: Synthesis and Application

RODNEY ANDREWS,* DAVID JACQUES, DALI QIAN, AND TERRY RANTELL

University of Kentucky Center for Applied Energy Research, 2540 Research Park Drive, Lexington, Kentucky 40511

Received March 4, 2002

ABSTRACT

Chemical vapor deposition (CVD) is the most promising synthesis route for economically producing large quantities of carbon nanotubes. We have developed a low-cost CVD process for the continuous production of aligned multiwall carbon nanotubes (MWNTs). Here we report the effects of reactor temperature, reaction time, and carbon partial pressure on the yield, purity, and size of the MWNTs produced. A simple method for purifying and healing structural defects in the nanotubes is described. The dispersion of nanotubes in polymer matrices has been investigated as a means of deriving new and advanced engineering materials. These composite materials have been formed into fibers and thin films and their mechanical and electrical properties determined.

Introduction

The discovery of carbon nanotubes (CNTs) in 1991[1] has stimulated intensive research to characterize their structure and to determine their physical properties both by direct measurement and through predictive methods using modeling techniques.[2,3] Many of their fundamental and remarkable properties are now well-known, and their exploitation in a wide range of applications forms a large part of the research effort now in progress. For example, their electronic properties[4] have already had a significant impact on field emission applications[5] in various electronic devices, while their geometry offers a new and exciting means of precision controlled drug delivery. However, it is their extraordinary mechanical properties[6] (exceptionally high tensile strength and stiffness) that has aroused particular interest and promoted research into the fabrication of nanotube composite materials. The lack of a reliable, large-volume production capacity, the high price of the nanotubes, and the fact that there is little selectivity in controlling the properties of the product are the three factors that have principally inhibited the commercialization of carbon nanotube technologies. Our interest at the University of Kentucky Center for Applied Energy Research has focused on the synthesis of multiwall carbon nanotubes (MWNTs) by a chemical vapor deposition (CVD) process designed to produce high-purity aligned nanotubes in bulk and at low cost. The bulk production of high-quality aligned MWNTs has allowed study of their dispersion in polymer matrices utilizing traditional polymer processing techniques and determination of the mechanical and electrical properties of the resulting composites.

Several of the enabling technologies required for nanotube applications are under development. For example, the ability to disperse individual MWNTs uniformly into a polymer matrix[7] and to control nanotube alignment within a composite material by shear field manipulation[8] has been demonstrated. One application likely to be implemented in the near term is the use of carbon nanotubes as fillers for controlling electrical properties of polymer systems. Carbon nanotubes could replace conventional conductive fillers in the formulation of conductive plastics for a range of applications. This is especially appealing as a much lower loading of carbon nanotubes can be used to achieve desired conductivity levels. Nanotube-loaded polymers are likely to see service as electromagnetic interference (EMI) and RFI shielding materials.[9,10] Recent advances in synthesis techniques, in particular CVD methods, show promise for being scalable (ton/day), low-cost (<$100/kg), and able to produce high product purity and selectivity. Only after bulk quantities of carbon nanotubes at low cost are available will they find common use in applications such as composite reinforced fibers or conductive plastics.

CVD Synthesis of MWNTs

Nanotube synthesis by a CVD process was chosen because it offers a promising route to bulk production of high-purity nanotubes that can be carried to commercialization. Useful composite research requires a bulk supply of nanotubes of high purity and in a useble (i.e., easily dispersible) form. Existing technologies for the production of single-wall nanotubes (SWNTs) do not yield sufficient quantities and lack the required purity. Purification of these materials is often tedious, low in yield, and damaging to the tubes' structure through oxidative shortening.[3,11] For applications such as conductive fillers or as reinforcing fibers, multiwall nanotubes are likely to be preferred over SWNTs on a cost basis. Also, technologies developed for MWNTs applications can be directly transferred to SWNT composites should SWNT synthesis reach industrial scale.

A synthesis method was developed to meet selected criteria: low cost, bulk production, high purity, and well-aligned (unentangled) product.[12] The system is relatively simple, consisting of a quartz tube reactor within a

Rodney Andrews is an Associate Engineer and Manager of the Carbon Materials Group at the University of Kentucky Center for Applied Energy Research. His current research interests include large-scale synthesis of carbon nanotubes, chemical modification of carbon nanotubes, nanotube composite materials, and applications of carbon nanotubes and activated carbons for gas separations.

David Jacques is a Research Associate at the University of Kentucky Center of Applied Energy Research. His current research interests are in the development and scaling of a carbon nanotube synthesis technique and the processing of nanotube/polymer and nanotube/pitch composites.

Dali Qian is a Post Doctoral Scholar in the University of Kentucky Center for Applied Energy Research. He is a member of the Microscopy Society of America (MSA) and the Microbeam Analysis Society (MAS). His major research interests include nanoscale materials, especially carbon nanotube CVD synthesis, characterizations, modifications, and their composite applications.

Terry Rantell is a Research Associate at the University of Kentucky Center for Applied Energy Research. His current areas of interest include the application of carbon nanotubes in the development of advanced composite materials.

10.1021/ar010151m CCC: $22.00
Published on Web 10/26/2002

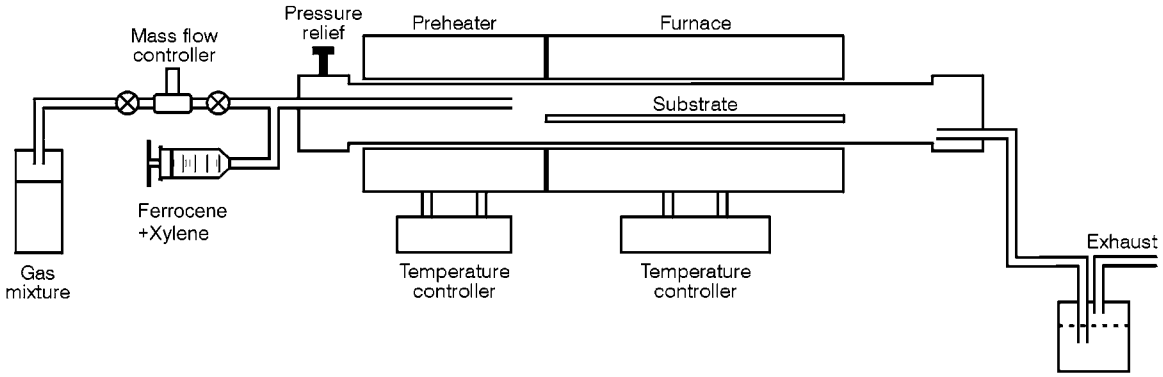

FIGURE 1. Schematic of floating catalytic CVD reactor system to produce MWNTs.

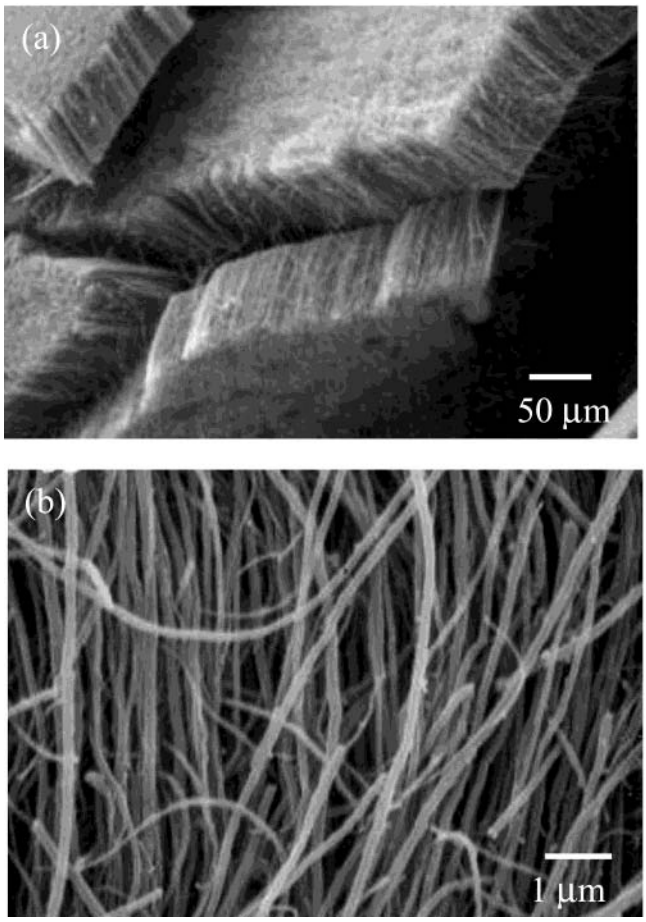

FIGURE 2. Typical well-aligned multiwall nanotube arrays from the floating catalytic CVD (a). Higher magnification shows alignment of nanotubes normal to the growth surface (b).

multizone furnace (Figure 1). The system configuration involves entraining a mixture of xylene and ferrocene (as suggested by Rao et al.[13,14]) into an inert gas stream. During the decomposition of the ferrocene−xylene mixtures at temperatures in the range 625−775 °C and at atmospheric pressure, iron nanoparticles are nucleated and begin to deposit carbon (from xylene and ferrocene) as well-aligned pure MWNT arrays on the quartz surfaces (reactor walls and substrates). Typical nanotube products, illustrating purity and alignment, are shown in Figure 2.

The control of tube diameter and length is a desirable feature of nanotube synthesis. Therefore, nanotube growth mechanisms and those factors determining the geometry of the product within the operating parameters of the reactor system have been studied. As the MWNT growth is initiated after the deposition of an Fe catalyst on the quartz surfaces, the production rate is directly proportional to the amount of surface area presented to the decomposing hydrocarbons. The MWNT growth appears to be instantaneous once a metal particle seeds on the substrate surface. From short-duration experiments (2−10 min), it appears that once growth initiates, the MWNTs rapidly grow to a maximum length (typically 50 μm).

A model to account for the growth mechanism of carbon nanotubes by catalytic decomposition of hydrocarbons has been proposed.[15] It was postulated that the formation and growth of nanotubes is an extension of other known processes in which graphitic structures are formed over metal surfaces at temperatures below about 1100 °C from carbon that is produced by the decomposition of a carbon-containing precursor. It was also proposed that the form of graphite that is produced is closely related to the physical dimensions of the metal catalyst particles. This hypothesis builds on a considerable volume of research that has been conducted over the past two to three decades on the formation of graphitic carbon over metal substrates.[16,17] The most effective metals have been shown to be iron, nickel, and cobalt.[18] The ability of these metals to form ordered carbons is thought to be related to a combination of factors, including (1) their catalytic activity for the decomposition of volatile carbon compounds, (2) the fact that they form metastable carbides, and (3) the fact that carbon is able to diffuse through and over the metals extremely rapidly.[16−18] The latter property allows ordered carbon to be produced by a mechanism of diffusion and precipitation. This also means that graphitic structures are formed only in proximity to the metal surface. If there is significant reaction away from the metal, other undesirable forms of carbon, such as amorphous carbon nanoparticles, will be co-produced. Restriction of the reaction to the surface is controlled through the choice of the carbon precursor, its partial pressure, and the reaction temperature.

A mass balance on the reactor gives a carbon yield of 20−80% for conversion of carbon to MWNTs, depending on the temperature and partial pressure of carbon (Figure 3). Interestingly, at higher reaction temperatures, larger

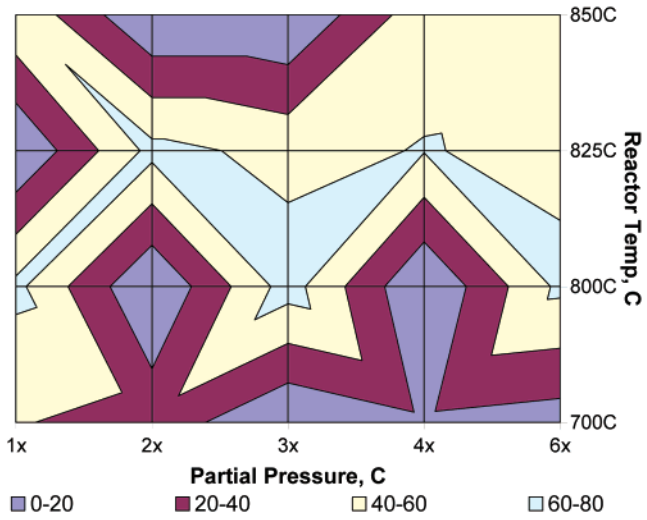

FIGURE 3. Operating envelope diagram showing carbon yield as a function of carbon partial pressure and reactor temperature. Yield as percent of carbon feed to reactor recovered in nanotube product. Partial pressure: 1× = 8 mbar, 6× = 48 mbar.

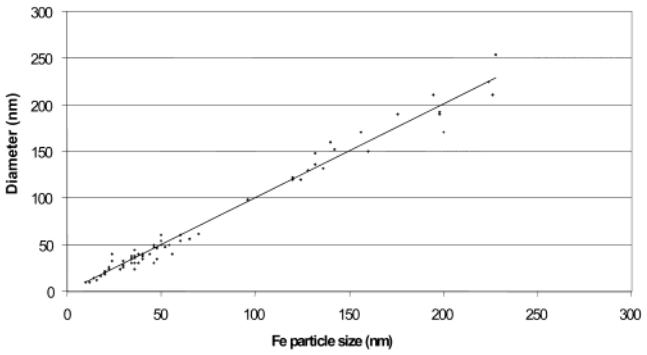

FIGURE 4. Correlation of nanotube outer diameter to the size of the metal catalyst particle, showing that the tube outer diameter is proportional to the catalyst particle size.

catalyst particles are produced that control the outer tube diameter (Figure 4). A systematic transmission electron microscopy (TEM) study of MWNTs synthesized at different reactor temperatures shows that the nanotube outer diameter is directly correlated to the catalyst particle size.[15] It should be noted that these larger diameter nanotubes do not lose the fine structure of concentric graphene cylinders (Figure 5). The larger diameter nanotubes simply consist of hundreds of shells and do not transform to one of the less well-ordered carbon structures (herringbone or platelet type nanofibers). High-resolution TEM images of MWNTs show the presence of the metal catalyst at the tip of the MWNTs. Predominately, the root ends of the MWNTs are found to be open.[12] Metal catalyst is also found within the core of the MWNTs in tests where high metal-to-carbon ratios (>0.0075) in the feed are used.

Changes in the carbon partial pressure in the feed affect the formation of co-generated amorphous carbon but have little effect on tube length. The production rate of MWNTs on the quartz substrates is shown as a function of the reactor temperature and partial pressure of carbon (1× = 8 mbar) in Figure 6. When varied over the range 8−48 mbar, optimum nanotube production rates were

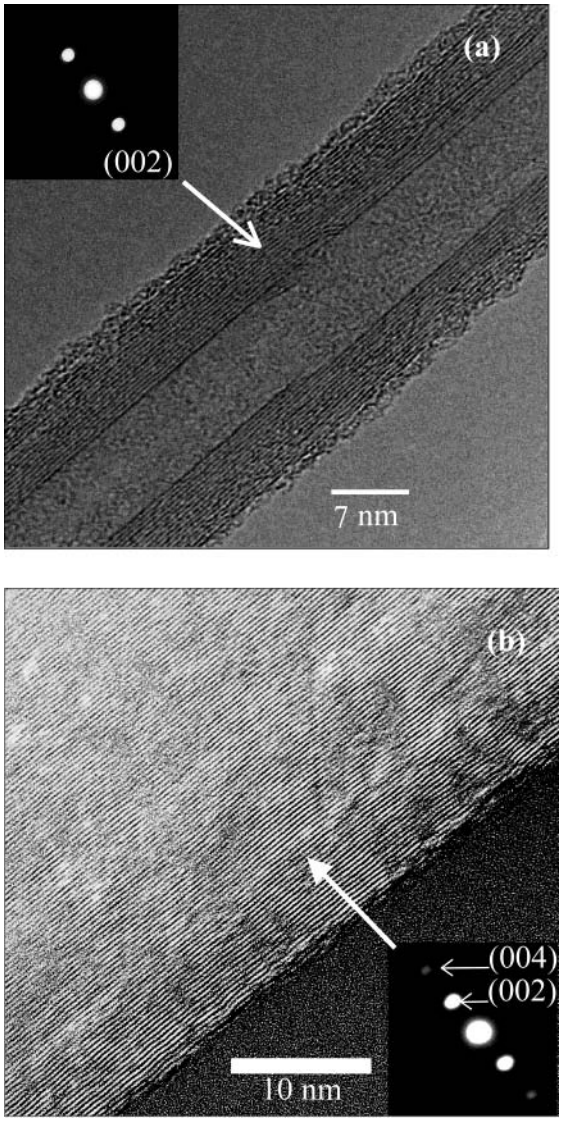

FIGURE 5. HRTEM images of MWNTs: (a) 18 nm diameter nanotube produced at 675 °C and (b) 180 nm diameter nanotube produced at 775 °C. The insets are the corresponding nanodiffraction patterns showing both tubes well-graphitized at low synthesis temperatures.

obtained at the low end of the range. This suggests that the carbon flux at the catalyst particle is also an important factor in determining the purity of carbon nanotubes. Clearly, in the temperature window of 800−825 °C, production rates as high as 1.5 g/m^2/min are achieved. Outside this range, a concomitant increase in the conversion of carbons into amorphous carbon was detected from the high-resolution scanning electron microscopy and TEM images.

Purification Methods

Nanotube synthesis by CVD has many advantages over other production routes, including the high purity of the product, which requires no further processing to yield a usable product. However, the significantly lower temperatures used in the synthesis, compared to those of arc or laser production methods, tend to produce nanotubes

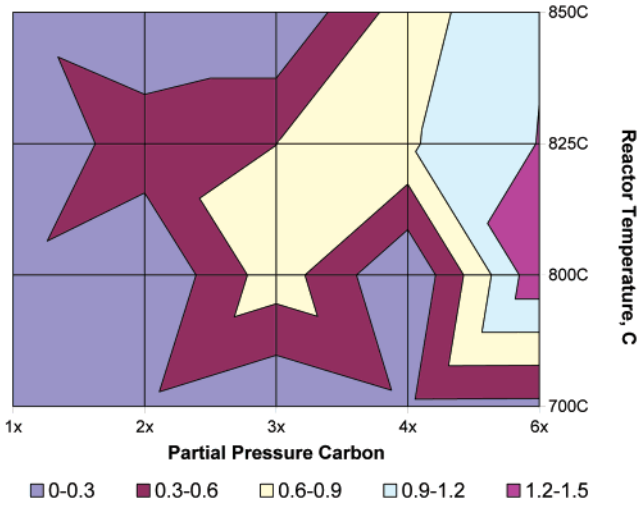

FIGURE 6. Operating envelope diagram showing nanotube production rate as a function of carbon partial pressure and temperature. Rate in grams per square meter per minute. Partial pressure: 1× = 8 mbar, 6× = 48 mbar.

with less well-defined graphene structure.[19] This can be rectified by a post-treatment in which the nanotubes are heated in an inert atmosphere to a high temperature in the range 1800−2600 °C. Not only does this graphitization process remove many of the structural defects, but it has also been shown to be a successful method for removing all of the residual iron catalyst.[20]

MWNT Composite Materials

The development of methods for the routine synthesis of carbon nanotubes has generated intense interest in exploiting their remarkable physical properties. The conductivity, strength, elasticity, toughness, and durability of formed composites may all be substantially improved by the addition of nanotubes. However, the effective utilization of carbon nanotubes in composite applications depends strongly on the ability to homogeneously disperse them throughout the matrix without destroying their integrity. Furthermore, good interfacial bonding is required to achieve load transfer across the CNT−matrix interface, a necessary condition for improving the mechanical properties of the composite. The very high aspect ratio of some carbon nanotubes may also enable them to be aligned with one axis of the composite. In other applications, their high axial electrical conductivity offers the potential for fabricating conducting polymers. To be cost-effective in such bulk applications, their projected performance must be realized at low concentrations.

Dispersion of the carbon nanotubes in the matrix is essential to achieving these objectives. In one approach, MWNTs have been dispersed into solutions of selected matrices using a high-energy ultrasonic probe.[7,21] The low viscosity of the solution allows the CNTs to move freely through the matrix. This was carried out in two stages, initially using a high-power ultrasonic probe to disperse the MWNTs in toluene. Subsequently, the dispersed suspension was mixed with a dilute solution (10 wt %) of polystyrene (PS) in toluene using an ultrasonic bath. This two-step approach was used to minimize the risk of tube rupture during processing and avoid disruption of the polymer structure by the powerful ultrasonic probe. The mixture was cast on glass and the solvent removed to yield MWNT-doped film.

The sonication approach is limited to matrices that freely dissolve in common solvents. It is therefore not particularly attractive for industrial-scale processes. A more practical method of producing MWNT/polymer composites involves shear mixing[22,23] followed by extrusion or injection molding to fabricate artifacts in the required form. The dispersion of carbon nanotubes in a range of polymers including high-impact polystyrene (HIPS), acrylonitrile−butadiene−styrene (ABS), and polypropylene (PP) has been investigated using a Haake Polylab High Shear Mixer. Tests were performed to determine the operating conditions required to disperse MWNTs; variables investigated included temperature, mixing time, rotor speed, and MWNT concentration. Test concentrations of up to 25 vol % were used to explore the effects on polymer performance at high loadings. For these tests, a master batch was prepared, and samples with lower concentrations were made by dilutition with fresh polymer. This approach minimizes the amount of MWNTs required but extends the processing time, which can be detrimental to the structure of the polymer.

Thin films have been prepared from the polymer/MWNT composite materials using a hydraulic press fitted with heated platens. In this procedure, a small sample of the crushed composite is loaded into a polytetrafluoroethylene (PTFE) vacuum bag. Metal shims are inserted between the platens to set a uniform separation. The envelope is evacuated, and once the sample has reached the required temperature, the sample is compressed into a film by applying a static load. Temperature, time, hydraulic pressure, and evacuation of the envelope are used to control film thickness and uniformity.

Fibers have been produced from the crushed composite materials by extrusion. The polymer/MWNT composite samples were transferred to a bench-scale extruder fitted with a 6.2 mm diameter screw and 0.3 mm diameter × 1 mm capillary die operating at 200 °C. The extruded thread was attached to a wind-up drum rotating at speeds of up to 1800 rpm to draw filament in the range 20−75 μm. The shear fields generated during spinning produce composite fibers with the MWNT aligned with the axis of the fiber (Figure 7).

Characterization. The films fabricated from the MWNT/polymer composite materials, each approximately 0.5 mm thick, were used in characterization studies. For the MWNT/polymer films, the standard measurement of the surface resistivity (ASTM D-257), ρ_s, is defined as the surface resistance multiplied by the ratio of the width of the electrodes to the distance between the electrodes, where the unit of ρ_s is Ω, or Ω/square (meaning the specimen surface dimensions: 1 cm × 1 cm, 1 m × 1 m, etc.). A Prostat POI-870 meter was used to measure surface resistivity in the range 10^3−10^{12} Ω/square, the limits of sensitivity of the meter. A wider range of measurements

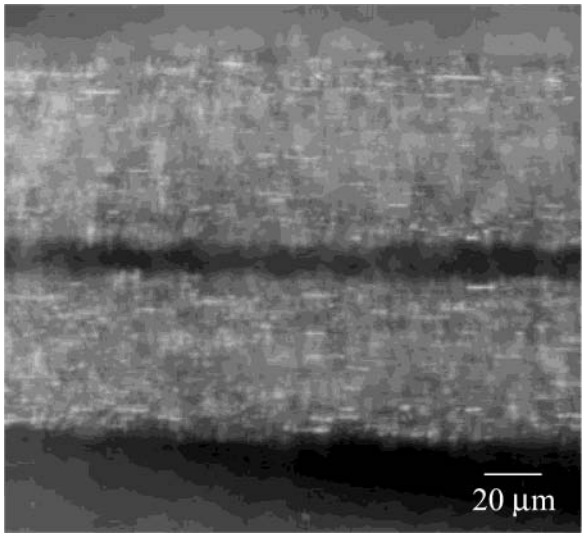

FIGURE 7. Typical optical micrograph of melt-spun MWNT/polymer fibers, showing the axial alignment of nanotubes.

was made at improved accuracy using a purpose built meter (concentric ring type) conforming to ASTM D257. The tensile strength and elastic modulus of samples cut from the films were measured using an MTS QT/1L tensile testing machine following ASTM D882 (for Young's modulus) and D638 (for tensile strength). Mechanical performance was also assessed by dynamic mechanical analysis (DMA) over the temperature range −100 to 150 °C. For Young's modulus and DMA analysis, strips were cut approximately 6 mm wide × 65 mm long, while dogbone samples were used for tensile strength. Test specimens were annealed at 120 °C for 15 h. The tensile properties of the composite fibers were measured following ASTM D3379.

Dispersion. Dispersion of the MWNTs after shear mixing was determined quantitatively using optical microscopy. Dispersion was assigned a value in the range 1−10, based upon the uniformity of nanotube distribution across the specimen and frequency of occurrence of agglomerates. Alternatively, inadequate dispersion may be represented by discontinuities at the boundaries between mixing zones containing different concentrations of dispersed MWNTs. Examples are illustrated in Figure 8. At any given temperature, dispersion efficiency is related to mechanical energy input into the mix (Figure 9). Increasing the residence time and/or the rotor speed can increase the energy input and hence improve the dispersion. Similar curves are produced when the temperature of the melt is changed or when a polymer with different melting characteristics is used. Higher energy input was required with increasing MWNT concentration due to an increase in melt viscosity.

Tube Fracture in Shear Mixing. High shear mixing to disperse MWNTs may result in tube breakage. For polystyrene with 0.5 vol % MWNTs, nanotube length distributions at regular intervals during mixing have been measured. Samples extracted from the mixer were diluted with acetone so that the recovered tubes could be deposited onto a TEM grid for analysis. The results (Figure 9) show

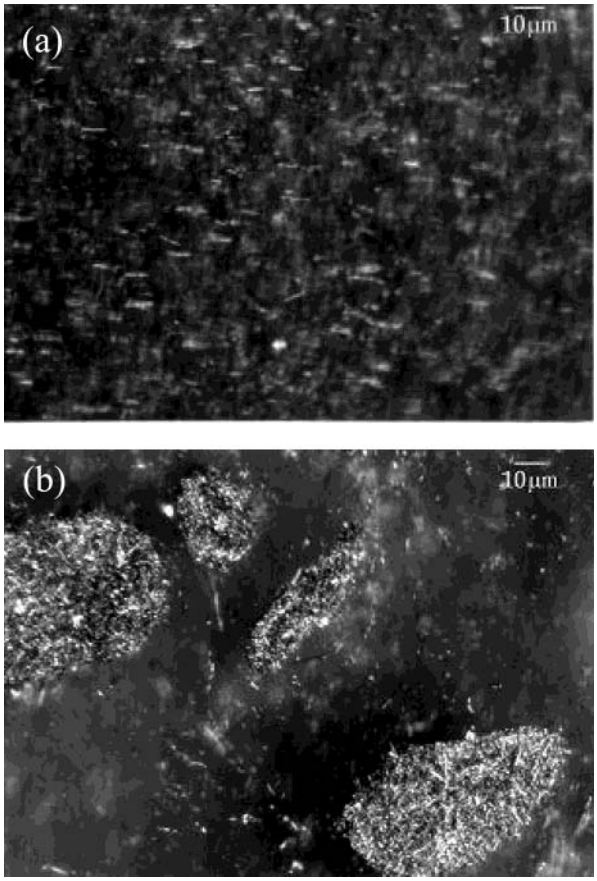

FIGURE 8. Typical optical micrograph illustrating good (uniform) (a) and poor dispersion (b), corresponding to high mixing energy and low mixing energy input into the shear mixing process.

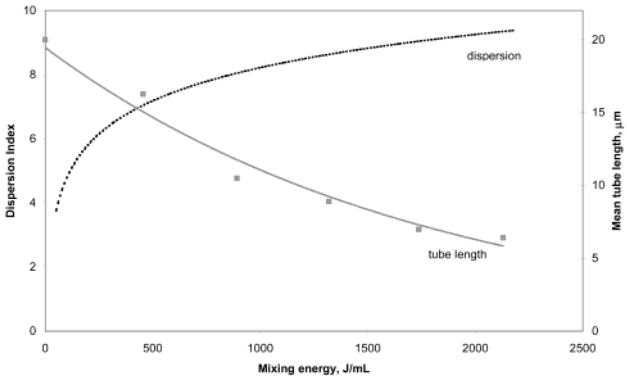

FIGURE 9. Relationship of nanotube dispersion and tube breakage after shear mixing. High shear mixing energy results in MWNT breakage and more uniform dispersion.

that some breakage does occur and that mean tube length decreases with increasing energy input. The rate at which mean tube length is reduced diminishes as the material is dispersed and tube separation increases. Hence, tube breakage is not a serious problem, the aspect ratio of the tubes remaining very high, reducing from 1000 to 250. Good dispersion can therefore be achieved at the expense of an acceptable reduction in tube length.

Surface Resistivity. The low-cost polymers used in the mass production of electronic components and devices are insulators, on which charge is able to accumulate with possible damage due to electrostatic discharge. Conduc-

tive filler addition is commonly used to induce conductivity for electrostatic charge control.[24,25] When mixed into molten polymer, filler particles form into chains or networks, providing conducting pathways. Carbon black is the most widely used filler material, although carbon fibers, metallic powders, and glass fibers coated with metals have also been used.[26] To attain the required electrical properties, the carbon black loading may be as much as 15−20 wt %, leading to particulate sloughing and loss of mechanical integrity.[27] These fillers also detract from the ability to recycle scrap materials, increasing waste disposal costs. Such fillers may also diminish other desirable properties of the polymer matrix, such as its light weight, its good mechanical toughness and strength, and its fabrication facility. Thus, the carbon black content must be minimized (to the percolation threshold) to retain these desirable properties and reduce costs.[28]

Carbon nanotubes offer the potential for fabricating conducting polymers without impairing the other polymer properties. Insulating materials have surface resistivity of $>10^{12}$ Ω/square. Protection against electrostatic discharge can be achieved by static dissipation if the surface resistivity of the polymer is in the range 10^5−10^{12} Ω/square, preferably at the low end of this range.[29−31] For electromagnetic interference screening, a more conductive polymer is required ($<10^5$ Ω/square). The addition of a small concentration of MWNTs to a polymer matrix can have a remarkable impact upon its electrical properties. At concentrations as low as 0.05 vol %, the surface resistivity of films fabricated using PP as the matrix fell from its virgin polymer value of $>10^{12}$ Ω/square to a value of $\sim10^5$ Ω/square, which indicates that the MWNT−PP film has a percolation threshold as low as 0.05 vol %. In contrast, the vapor-grown carbon fiber (VGCF, with diameter of 200 nm)−PP composite has a percolation threshold of 3 vol %, while the carbon black epoxy has a percolation threshold as high as 10 vol %.[32] Increasing the MWNT concentration resulted in a progressive decrease in resistivity. With polystyrene or its high-impact variant (HIPS) as the matrix, similar results were found when low concentrations of MWNTs were introduced. However, for the ABS matrix, the addition of up to 0.5 vol % MWNT had little effect upon surface resistivity, perhaps an indication of segregation of the MWNTs into a particular phase but lacking continuity through the matrix. At higher MWNT concentrations, the surface resistivity of the MWNT−PS and MWNT−PP films falls to <100 Ω/square (Figure 10), approaching the value for pure carbon black or metals.

Tensile Properties. While the dispersion of low concentrations (<0.5 vol %) of MWNTs into the selected polymers produced a remarkable reduction in surface electrical resistivity, their effect on the tensile properties was relatively small. There was generally a small increase in elastic modulus and a decrease in tensile strength. This reduction in tensile strength can be attributed to an increase in the frequency distribution of defects associated with the nanotubes that initiate failure. Poor interfacial bonding between the nanotubes and the matrix will also have a significant influence on the mechanical properties

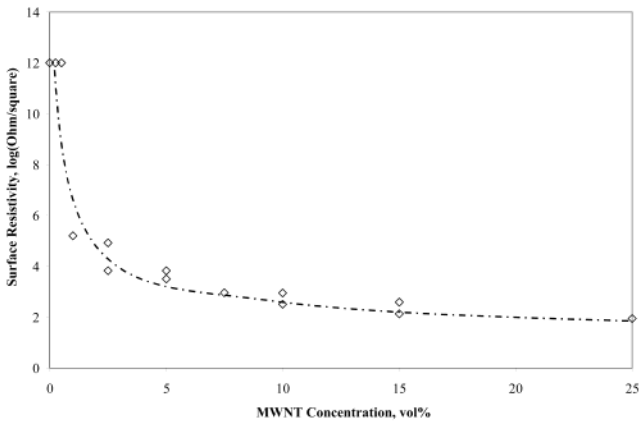

FIGURE 10. Surface electrical resistivity of MWNT/PS and MWNT/PP composite films with varying MWNT concentration.

of the films. This allows fiber pull-out and consequent failure of the film. A possible remedy is to modify the surface character of the carbon nanotubes. A number of surface treatment methods, including functionalization techniques, are being considered for this purpose.

When a tensile stress is applied to the MWNT−PS film using a straining TEM holder, a crack can be nucleated around a notch due to stress concentration. In situ TEM observations of the crack propagation through the PS matrix show that the MWNTs tend to align along the tensile direction and bridge the crack faces in the wake. These bridging nanotubes provide closure stresses across the crack faces and reduce the stress concentration around the crack tip. In Figure 11, even though the crack opening displacement exceeds 500 nm, the well-bonded cluster of nanotubes at the center of the image (Figure 11b) locally retards crack opening in the composite. Eventually, as shown in Figure 11c, the nanotubes debond and are pulled out of the matrix. Some tubes have broken at obvious defects, such as an Fe catalyst particle. Annealing the CNTs at high temperatures (>2200 °C) can be done to remove the Fe catalyst inclusions and other defects and potentially increase the strength of the CNTs and the composites derived from them.

At higher MWNT concentrations, the changes in the mechanical properties of the films are more pronounced. For polystyrene/MWNT composites containing from 2.5 to 25 vol % MWNTs, Young's modulus increased progressively from 1.9 to 4.5 GPa, with the major increases occurring when the MWNT content was at or above about 10 vol % (Figure 12). However, the dependence of tensile strength on MWNT concentration is more complex. At the lower concentrations (≤10 vol %), the tensile strength decreases from the neat polymer value of ∼40 MPa, only exceeding it when the MWNT content is above 15 vol % (Figure 12). When the structural imperfections and impurities present in the as-prepared MWNTs are removed by heating to graphitization temperatures, the polystyrene/MWNT composites made from them show improved performance. Here, although the tensile strength again initially falls at low MWNT concentrations, the recovery in strength occurs at much lower MWNT concentrations (∼5 vol %) than for the untreated nanotubes, and there-

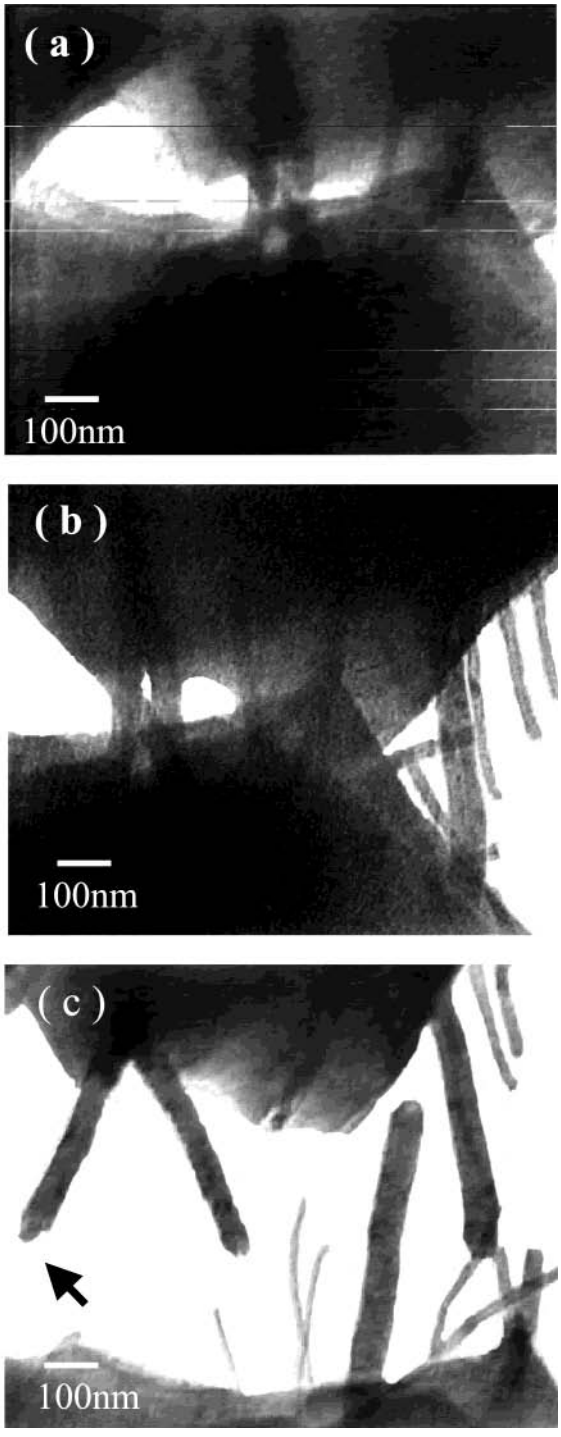

FIGURE 11. Real-time TEM observations of MWNT/PS deformation under tension on a straining TEM holder, showing that MWNTs prevent crack opening.

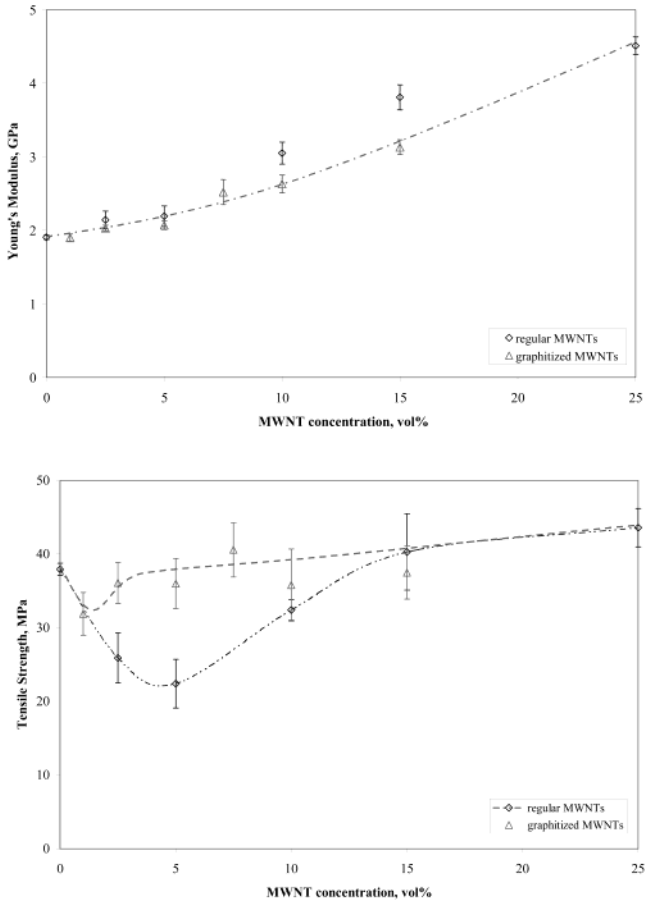

FIGURE 12. Tensile properties of polystyrene/MWNT composite films with various MWNT concentrations, obtained by shear mixing followed by hot press.

after increases further as the concentration is raised. Young's modulus increases progressively with graphitized MWNT concentration, in a manner similar to the composite films prepared from the regular MWNTs. The random but well-dispersed distribution of MWNTs in polypropylene is illustrated in the tensile fracture surfaces (Figure 13). The effectiveness of load transfer from the matrix to the nanotube reinforcements is determined by the interfacial bonding strength, which depends strongly on three factors:[33] micromechanical interlocking, van der Waals adhesion, and chemical bonding between the fillers and polymer matrices. Molecular mechanics calculations[34] show that the sliding frictions between nanotube−polymer interfaces are much higher than that between neighbor layers of a MWNT, and these frictional forces play only a minor role in determining the interface strength. The van der Waals forces, arising mainly from the hydrogen bond interactions between the π-bonds of MWNT surface and the hydroxy side groups of the polymer matrix, are determined by the polymer molecular structure, especially its ability to form ordered helices around individual nanotubes.[34] For our MWNT/polymer composite, with average tube diameters of 33 nm (MWNTs grown at 700 °C), it is not clear if the polymer chains can form large enough helices to wrap around the MWNTs. The high-temperature annealing of CVD-derived MWNTs removes the residual catalyst and other structural defects to increase the strength of the NTs. However, the high-temperature treatment also removes the tube surface active sites to reduce the polymer−MWNT interfacial bonding. The competition between the two factors determines the final load transfer effect. The experimental results (Figure 12) show that high-temperature annealing increases the PS−MWNT interfacial bonding strength. Suitable surface functionalizations of tubes increase the NT−polymer interfacial adhesion and chemical bonding,

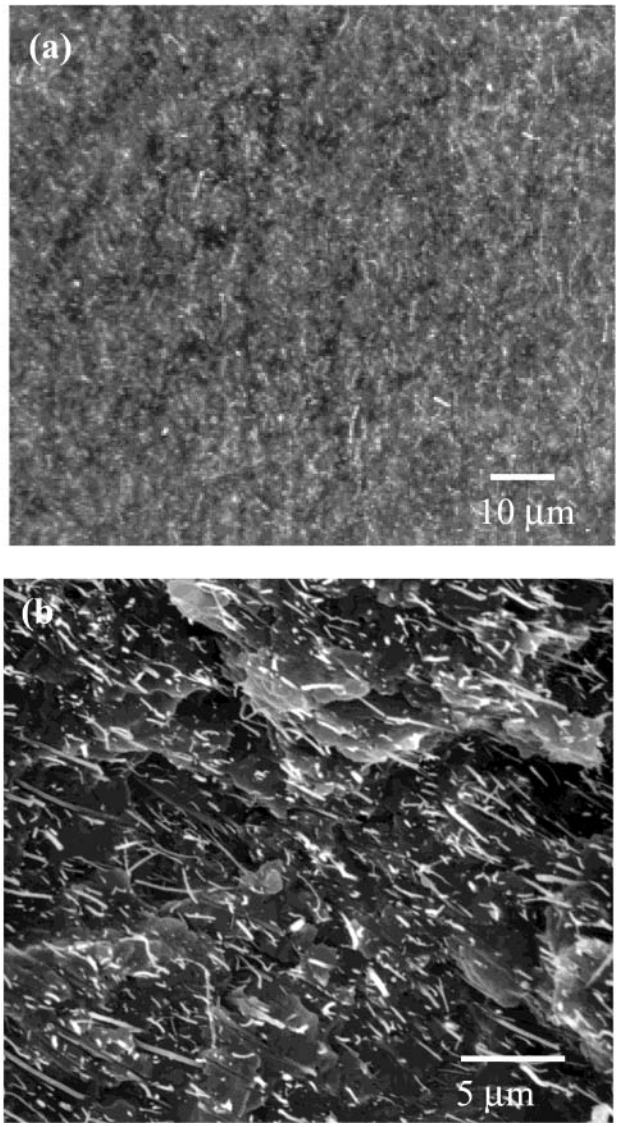

FIGURE 13. Well-dispersed MWNTs in a polypropylene matrix after shear mixing. Optical micrograph of cast thin film (a) and SEM image of the fracture surface of the MWNT/PP film after tensile test (b).

and further realize effective load transfer to the nanotubes. The selections of matrix polymer and suitable MWNT surface functionalizations are the key issues to be addressed in producing multifunctional NT−polymer advanced composites.

DMA measurements are consistent with the tensile test data. These show that there is a progressive increase in storage and loss modulus with increasing MWNT concentration over the temperature range −100 to 150 °C, with the biggest increase occurring at concentrations of ≅10 vol % (Figure 14). The value of tan δ decreases progressively with MWNT concentration (Figure 14). In addition, the temperature at which a step transition from elastic to plastic deformation occurs increases with increasing MWNT content, and there are similar and corresponding increases in the onset of the loss modulus and tan δ peaks (Figure 15). In general, as the MWNT content rises, the temperature dependence of the physical properties of the composites decreases.

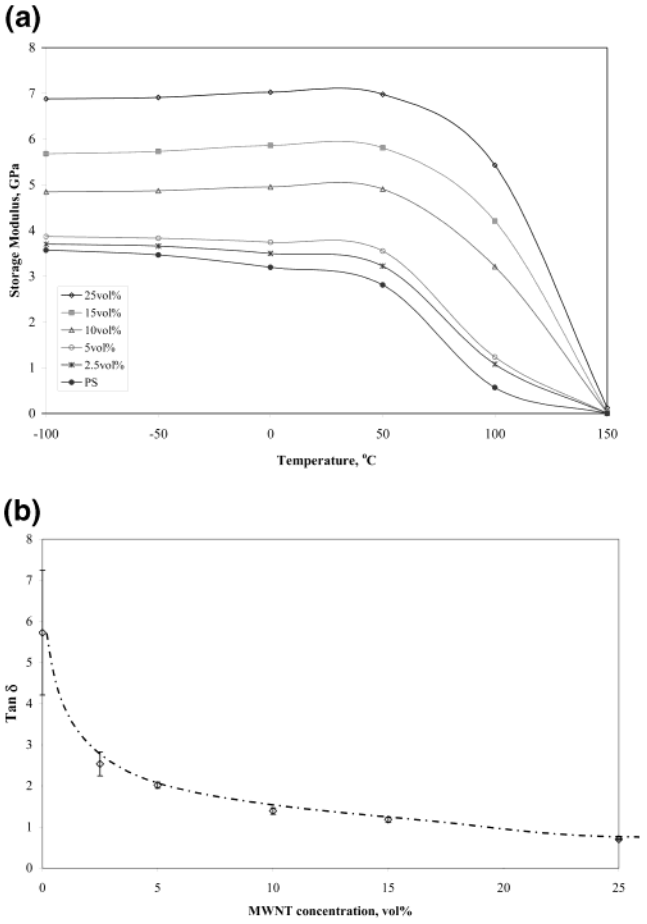

FIGURE 14. Characterization of MWNT/PS films by DMA measurement: (a) storage modulus increases and (b) tan δ decreases with increasing MWNT loading.

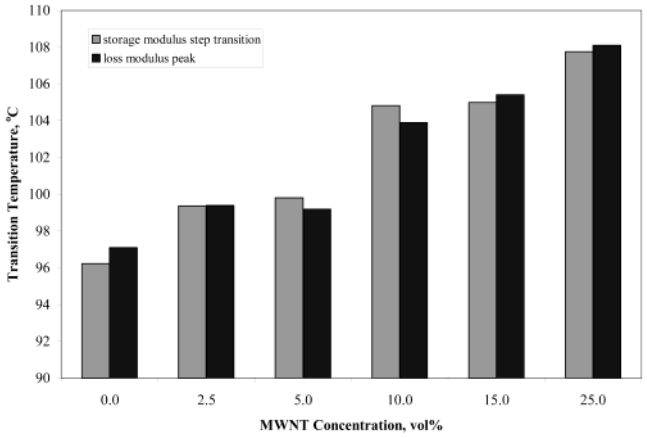

FIGURE 15. Transition temperatures (storage modulus step transition and loss modulus peak) are shifted upward with increasing MWNT loading.

Polymer/MWNT Composite Fibers

The tensile properties of fibers produced from the polymer/MWNT composites follow similar trends. For example, polypropylene/MWNT composite fibers exhibit a significant increase in elastic modulus with increasing MWNT concentration, but no improvement in tensile strength. At low MWNT concentrations, the tensile strength, largely

controlled by the distribution of flaws, diminishes, due to an increase in the frequency distribution of defects associated with the nanotubes ends. Although the nanotubes have a very high aspect ratio of ~1000, they are relatively short, ~20 μm, and hence on a macro scale do not act as continuous reinforcing phases typical in high-performance fiber-reinforced composites. Moreover, if the interfacial adhesion is poor, it results in premature composite failure since the reinforcing nanotubes simply pull out of the matrix without contributing to the strength or stiffness of the material. At higher concentrations, there are more interactions between the MWNTs, and crack propagation is inhibited, resulting in increased tensile strength observed for the composite films. This is further improved when defects in the nanotubes structure are removed by annealing at high temperatures. However, there are some significant differences in the physical properties of the fibers in comparison to the composite films. Young's modulus is significantly increased at lower MWNT concentrations in the fibers (<2.5 vol %). This results from the axial alignment of the nanotubes in the fibers. The method of fabrication of the films does not promote significant orientation of the MWNTs in a preferred direction, the distribution being essentially random. There is no unidirectional shear field in the processing to cause alignment, unlike artifacts produced by extrusion through a narrow die (e.g., fibers or extruded film). Substantial gains in the mechanical properties of both films and fibers may be expected upon making improvements to the interfacial bonding between the MWNTs and the polymer matrix.

A further manifestation of the different nanotube distribution is shown by the electrical conductivity measurements. The surface conductivity of the composite films occurs at very low MWNT concentrations, whereas the fibers retain their insulating properties up to relatively high MWNT concentrations (~10 vol %). The random distribution of the MWNTs in the films results in the formation of conducting pathways through the material, while in the fibers there is little contact between the nanotubes at low loadings. The MWNTs within the fibers are well-dispersed and aligned with the fiber axis. Hence, at low concentrations there is less probability of the MWNTs forming a continuous conducting path along the length of the composite fiber.

Conclusions

Realization of the extraordinary properties presented by carbon nanotubes holds much promise to revolutionize several fields, and we are tantalizingly close to achieving these remarkable changes. We have developed a low-temperature CVD process for the production of aligned, high-purity multiwall carbon nanotubes. The process has production rates up to 1.5 g m^{-2} min^{-1}, with carbon yields approaching 70% conversion of all carbon fed to MWNT product. While the process produces nanotubes of high purity, 5% iron catalyst remains in the tubes. Graphitization is an effective way to both remove the catalyst and anneal out structural defects in the nanotubes.

MWNTs can be uniformly dispersed into polymers to produce significant changes to the physical properties of the host matrix. A small but acceptable amount of tube breakage may occur. The dispersion of low concentrations (<0.5 vol %) of MWNTs in a polymer matrix resulted in substantial decreases in the electrical surface resistivity of the derived composite material. In polypropylene, the inclusion of only 0.05 vol % MWNTs produced a reduction in resistivity from $>10^{12}$ to $\sim10^{5}$ Ω/square, and higher concentrations produced further reductions to <100 Ω/square.

Low concentrations of MWNTs in polymer matrices resulted in an increase in Young's modulus and a reduction in the tensile strength. At higher concentrations, both stiffness and strength were significantly improved. Removal of defects and impurities from the nanotubes by graphitization further improves the tensile properties of the composites. Analysis of the tensile failure mechanism suggests that surface treatment of the nanotubes could be used to improve interfacial bonding and increase tensile strength. When interfacial adhesion is poor, the nanotubes pull out of the matrix. Good adhesion results in nanotube crack bridging and ultimate failure of the nanotube. Controlling this failure mechanism will be instrumental to achieving true superstrong materials based on carbon nanotubes.

The authors acknowledge financial support from the NSF MRSEC Advanced Carbon Materials Center at University of Kentucky (NSF-MRSEC Grant DMR-9809686).

References

(1) Iijima, S. Helical microtubules of graphitic carbon. *Nature* **1991**, *354*, 56−58.
(2) Harris, P. J. F. *Carbon nanotubes and related structures: New materials for the 21st Century*; Cambridge University Press: New York, 1999.
(3) Sinnott, S. B.; Andrews, R. Carbon Nanotubes: Synthesis, properties and applications. *Crit. Rev. Solid State Mater. Sci.* **2001**, *26*, 145−249.
(4) Dresselhaus, M. S.; Dresselhaus, G.; Eklund, P. C. *Science of fullerenes and carbon nanotubes*; Academic Press: San Diego, 1996.
(5) Rao, A. M.; Jacques, D.; Haddon, R. C.; Zhu, W.; Bower, C.; Jun, S. In situ-grown carbon nanotube array with excellent field emission characteristics. *Appl. Phys. Lett.* **2000**, *76*, 3813−3815.
(6) Wong, E. W.; Sheehan, P. E.; Lieber, C. M. Nanobeam mechanics: Elasticity, strength, and toughness of nanorods and nanotubes. *Science* **1997**, *277*, 1971−1975.
(7) Qian, D.; Dickey, E. C.; Andrews, R.; Rantell, T. Load transfer and deformation mechanisms in carbon nanotube-polystyrene composites. *Appl. Phys. Lett.* **2000**, *76*, 2868−2870.
(8) Andrews, R.; Minot, M.; Jacques, D.; Rantell, T. Processing of nanotube-polymer composites by shear mixing. *Macromol. Mater. Eng.* **2002**, *287*, 395−403.
(9) Grimes, C. A.; Mungle, C.; Kouzoudis, D.; Fang, S.; Eklund, P. C. The 500 MHz to 5.50 GHz complex permittivity spectra of single-wall carbon nanotube-loaded polymer composites. *Chem. Phys. Lett.* **2000**, *319*, 460−464.
(10) Grimes, C. A.; Dickey, E. C.; Mungle, C.; Ong, K. G.; Qian, D. The effect of purification on the electrical conductivity and complex permittivity of multiwall carbon nanotubes. *J. Appl. Phys.* **2001**, *90*, 4134−4137.
(11) Ebbesen, T. W. In *Carbon nanotubes: Preparation and properties*; Ebbesen, T. W., Ed.; CRC Press: Boca Raton, 1997; pp 226−248.
(12) Andrews, R.; Jacques, D.; Rao, A. M.; Derbyshire, F.; Qian, D.; Fan, X.; Dickey, E. C.; Chen, J. Continuous production of aligned carbon nanotubes: A step closer to commercial realization. *Chem. Phys. Lett.* **1999**, *303*, 467−474.

(13) Sen, R.; Govindaraj A.; Rao, C. N. R. Carbon nanotubes by the metallocene route. *Chem. Phys. Lett.* **1997**, *267*, 276−280.
(14) Rao, C. N. R.; Sen, R.; Satishkumar, B. C.; Govindaraj A.; Large aligned-nanotube bundles from ferrocene pyrolysis. *Chem. Commun.* **1998**, 1525−1526.
(15) Sinnott, S. B.; Andrews, R.; Qian, D.; Rao, A. M.; Mao, Z.; Dickey, E. C.; Derbyshire, F. Model for carbon nanotube growth through chemical vapor deposition. *Chem. Phys. Lett.* **1999**, *315*, 25−30.
(16) Baker, R. T. K.; Harris, P. S. In *Chemistry and Physics of Carbon*; Walker, P. L., Thrower, P. A., Eds.; Marcel Dekker: New York, 1978; Vol. 14, p 83.
(17) Baker, R. T. K. Catalytic Growth of Carbon Filaments. *Carbon* **1989**, *27*, 315−323.
(18) Derbyshire, F.; Presland, A. E. B.; Trimm, D. L. Graphite formation by the dissolution-precipitation of carbon in cobalt, nickel and iron. *Carbon* **1975**, *13*, 111−113.
(19) Ebbesen, T. W. In *Carbon nanotubes: Preparation and properties*; Ebbesen, T. W., Ed.; CRC Press: Boca Raton, 1997; pp 139−162.
(20) Andrews, R.; Jacques, D.; Qian, D.; Dickey, E. C. Purification and Structural Annealing of Multiwalled Carbon Nanotubes at Graphitization Temperatures. *Carbon* **2001**, *39*, 1681−1687.
(21) Andrews, R.; Jacques, D.; Rao, A. M.; Rantell, T.; Derbyshire, F.; Chen, Y.; Chen, J.; Haddon, R. C. Nanotube composite carbon fibers. *Appl. Phys. Lett.* **1999**, *75*, 1329−1331.
(22) Lozano, K.; Barrera, E. V. Nanofiber-reinforced thermoplastic composites. I. Thermoanalytical and mechanical analyses. *J. Appl. Polym. Sci.* **2001**, *79*, 125−133.
(23) Haggenmueller, R.; Gommans, H. H.; Rinzler, A. G.; Fischer, J. E.; Winey, K. I. Aligned single-wall carbon nanotubes in composites by melt processing methods. *Chem. Phys. Lett.* **2000**, *330*, 219−225.
(24) Narkis, M.; Lidor, G.; Vaxman, A.; Zuri, L. *Conducting Polymers and Plastics*; Plastics Design Library: New York, 1999; pp 209−217.
(25) Street, G. B. *Handbook of Conducting Polymers*; Marcel Dekker: New York, 1986; Vol. 1.
(26) Tchoudakov, R.; Breuer, O.; Narkis, M.; Siegmann, A. Conductive polymer blends with low carbon black loading: polypropylene/polyamide. *Polym. Eng. Sci.* **1996**, *36*, 1336−1346.
(27) Donnet J.-B.; Bansal R. C.; Wang, M.-J. *Carbon Black: Science and Technology*; Marcel Dekker: New York, 1993.
(28) Broadbent, S. R.; Hammersley, J. M. Percolation process. I. Crystals and mazes. *Proc. Cambridge Philos. Soc.* **1957**, *53*, 629−41.
(29) Scobbo, J. J. In *ANTEC Proceedings*; Society of Plastics Engineers: Atlanta, 1998; Vol. 2, pp 2468−2472.
(30) Campbell, R.; Tan, W. In *Electrical Overstress/Electrostatic Discharge Symposium Proceedings*; Reliability Analysis Center: Griffiss AFB, NY; 1995; p 218.
(31) Vakiparta, K.; Kirmanen, P.; Laasko, J.; Passiniemi, P.; Taka, T.; Virtanen, E. In *Electrical Overstress/Electrostatic Discharge Symposium Proceedings*; Reliability Analysis Center: Griffiss AFB, NY, 1995; pp 229−235.
(32) Finegan, I. F.; Tibbetts, G. G. Electrical conductivity of vapor-grown carbon fiber/thermoplastic composites. *J. Mater. Res.* **2001**, *16*, 1668−1674.
(33) Schadler, L. S.; Giannaris, S. C.; Ajayan, P. M. Load transfer in carbon nanotube epoxy composites. *Appl. Phys. Lett.* **1998**, *73*, 3842−3844.
(34) Lordi, V.; Yao, N. Molecular mechanics of binding in carbon-nanotube−polymer composites. *J. Mater. Res.* **2000**, *15*, 2770−2779.

AR010151M